Frontiers in Bioscience Landmark

Front. Biosci. (Landmark Ed) **2026**; 31(2): 46689
https://doi.org/10.31083/FBL46689

Original Research

Electroacupuncture Facilitates the Regulation of Inflammation in the Conjunctiva of Rabbits With Dry Eye Syndrome via the α7nAChR-HMGB1 Signaling Pathway

Ning Ding[1,2,†], Jie Zhang[2,†], Xia Wu[1], Shangjie Liang[1], Dandan Zhu[3], Mengting Huan[1,4], Lizhen Gan[1], Yunfeng Wu[1], Huxing Shen[5], Tengyan Ji[6], Yunchuan Wu[1,*], Qingbo Wei[1,*]

[1]School of Acupuncture-Moxibustion and Tuina, Nanjing University of Chinese Medicine, 210023 Nanjing, Jiangsu, China
[2]Yizheng Clinical School, Jiangsu Health Vocational College, 211400 Yangzhou, Jiangsu, China
[3]Department of Ophthalmology, Nanjing Drum Tower Hospital, The Affiliated Hospital of Nanjing University Medical School, 210000 Nanjing, Jiangsu, China
[4]Now with Rehabilitation Department, Xuzhou Tongshan District Hospital of Traditional Chinese Medicine, 221100 Xuzhou, Jiangsu, China
[5]Department of Ophthalmology, Affiliated Hospital of Nanjing University of Chinese Medicine, 210029 Nanjing, Jiangsu, China
[6]Traditional Chinese Medicine Rehabilitation Center, The Second Affiliated Hospital of Nanjing University of Chinese Medicine, 210017 Nanjing, Jiangsu, China
*Correspondence: 270847@njucm.edu.cn (Yunchuan Wu); 270762@njucm.edu.cn (Qingbo Wei)
†These authors contributed equally.
Academic Editor: Dario Rusciano
Submitted: 17 September 2025 Revised: 8 December 2025 Accepted: 19 January 2026 Published: 12 February 2026

Abstract

Background: Altered homeostasis of the ocular surface microenvironment is a hallmark of dry eye disease (DED). The alpha-7 nicotinic acetylcholine receptor (α7nAChR) plays a key role in DED pathophysiology. In this study, we established a rabbit model of DED using scopolamine hydrobromide (Scop) to determine the effect of electroacupuncture (EA) on ocular surface damage in DED and to explore its underlying mechanisms. **Methods**: New Zealand White rabbits (1.5–2.0 kg) were subcutaneously administered Scop for 21 days prior to EA treatment. After 35 days, the homeostasis of the ocular surface microenvironment was evaluated using the Schirmer I test (SIT), tear break-up time (BUT), corneal fluorescein (FL) staining, and measurement of tear osmolarity. The expression levels of ACh, α7nAChR, and high mobility group box 1 (HMGB1) were detected via histopathological examination of the cornea, lacrimal glands, and conjunctiva, combined with immunohistochemistry and western blotting. Additionally, protein chip technology was used to determine the expression levels of downstream factors. **Results**: EA stimulation significantly improved the homeostasis of the ocular surface microenvironment, as evidenced by increased SIT values and BUT, reduced corneal FL intensity, and decreased tear osmolarity. It also alleviated pathological damage to the cornea, conjunctiva, and lacrimal glands; upregulated the expression of ACh and α7nAChR; and downregulated the expression of HMGB1 and related inflammatory factors. However, these changes were reversed following administration of α-Bungarotoxin. **Conclusion**: EA stimulation improves ocular surface homeostasis and reduces inflammation in DED, potentially via activation of the α7nAChR signaling pathway, which in turn inhibits the expression of HMGB1 and inflammatory factors.

Keywords: electroacupuncture; dry eye; inflammation; alpha-7 nicotinic acetylcholine receptor; high mobility group box 1

1. Introduction

Dry eye disease (DED) is a prevalent multifactorial ocular surface disorder triggered by factors such as pharmaceutical use, hormonal imbalance, corneal refractive surgery, systemic diseases, and allergic reactions [1]. These etiologies disrupt tear film stability and homeostasis, initiating a self-perpetuating cycle of ocular surface inflammation and damage to the ocular surface microenvironment [2]. Clinical manifestations include dryness, foreign body sensation, burning, and blurred vision, which significantly impair patients' quality of life [3,4]. Current therapeutic strategies for DED only provide transient symptomatic relief. Long-term use of corticosteroids may cause ocular surface damage, while cyclosporine-A ophthalmic emulsion requires several weeks to months to take effect and exhibits limitations in inhibiting innate pro-inflammatory mediators [5]. Thus, there is an urgent need to develop safer and more effective therapeutic approaches for DED.

Electroacupuncture (EA), a key therapeutic modality in traditional Chinese medicine, involves delivering electrical stimulation to specific acupoints with adjustable frequency and intensity to modulate neurological, immunological, and other physiological functions [6,7]. As a safe and cost-effective intervention, EA exerts anti-inflammatory effects and is recommended for restoring homeostatic balance [7–10]. Studies have confirmed the efficacy, safety,

and feasibility of EA in improving DED symptoms and signs, with significant enhancements in the Ocular Surface Disease Index (OSDI), Schirmer I test (SIT) scores, and tear film break-up time (BUT) [11,12]. Our previous research verified that EA can suppress inflammation in the cornea and lacrimal glands, potentially through vagus nerve-mediated regulation of neuroimmune responses to inhibit inflammatory reactions [13,14]. As previously reported, EA can activate the cholinergic anti-inflammatory pathway [15].

This pathway is initiated by the binding of acetylcholine (ACh)—released from the vagus nerve—to the alpha-7 nicotinic ACh receptor (α7nAChR), which subsequently inhibits the release of downstream pro-inflammatory factors. This mechanism contributes to the treatment of inflammatory diseases and alleviates immune dysregulation associated with such conditions [15–18]. Furthermore, accumulating evidence has demonstrated that α7nAChR is expressed in conjunctival epithelial cells and lacrimal gland acinar cells, and its activation can reduce the secretion of pro-inflammatory cytokines in response to ocular surface injury [15,19]. Activation of α7nAChR can inhibit the high-mobility group box 1 (HMGB1)/nuclear factor kappa B (NF-κB) pathway, ameliorating radiation-induced lung injury, zymosan-induced acute kidney injury, and post-anesthetic cognitive impairment [20–22].

HMGB1, a non-histone nuclear protein belonging to the damage-associated molecular pattern family, has been detected in the tear fluid of patients with ocular surface inflammatory conditions such as conjunctivitis, blepharitis, and DED [19]. Under quiescent conditions, HMGB1 is localized intracellularly as an inflammatory mediator; however, its extracellular release can activate the innate immune response, triggering a pro-inflammatory vicious cycle that sustains immune activation and contributes to tissue damage.

To date, the mechanism underlying the role of the α7nAChR-HMGB1 signaling pathway in EA-mediated effects on conjunctival tissue in scopolamine hydrobromide (Scop)-induced rabbit models of DED remains unclear. Therefore, this study determined whether EA exerts its effects on conjunctival tissue in DED rabbits via the α7nAChR-HMGB1 signaling pathway, thereby alleviating ocular surface inflammation and damage.

2. Materials and Methods

2.1 Animals

Adult New Zealand white rabbits (1.5–2.0 kg) were purchased from the Qinglong Mountain Experimental Animal Center (No. SCXK Jiangsu 2024-0001; Nanjing, China) and housed in the Pharmacology Animal Laboratory of Jiangsu Province Hospital of Traditional Chinese Medicine (Jiangsu, China). Housing conditions were maintained at a constant temperature of 22 °C $\pm$ 2 °C, relative humidity of 60% $\pm$ 5%, and a 12-hour light/dark cycle, with ad libitum access to food and water. Experimental rabbits were humanely euthanized via intravenous injection of sodium pentobarbital (120 mg/kg; 50 mg/mL) into the marginal ear vein. Death was confirmed by $\geq$3 minutes of absent heartbeat (auscultation), loss of corneal reflex, and fixed dilated pupils. All procedures were performed by trained personnel in a dedicated room to minimize animal stress.

2.2 Dry Eye Model Induction

The DED model was established by subcutaneous injection of Scop at the nape of the neck (Fig. 1A) at a dose of 2.0 mg/kg per injection, administered four times daily (8:00, 11:00, 14:00, and 18:00) for 21 consecutive days. Successful model establishment was confirmed by strong positive corneal fluorescein (FL) staining (Fig. 1B).

2.3 Experimental Grouping

Experiment 1: Male adult New Zealand white rabbits were randomly divided into four groups (n = 6 per group): (1) Vehicle control group; (2) Scop group; (3) Scop + sham group; and (4) Scop + EA group. Experiment 2: Adult New Zealand white rabbits of both sexes were randomly divided into five groups (n = 6 per group): (1) Vehicle control group; (2) Scop group; (3) Scop + EA group; (4) Scop + α-BGT + EA group; and (5) Scop + α-BGT group.

EA treatment was initiated on day 22 and administered once daily for 14 consecutive days. For the Scop + sham EA group, blunt needle puncture at acupoints was performed daily from day 22 for 14 days. A selective α7nAChR antagonist, α-Bungarotoxin (α-BGT, pk-ca707-00010-1; Germany), was administered via the ear vein at a dose of 4.0 µg/kg daily from day 22 for 14 days. The vehicle control group received subcutaneous injections of 0.9% sodium chloride according to the same schedule and dosage as the Scop-treated groups for a total of 35 days.

2.4 EA Stimulation

EA stimulation was performed using the Hwato Electronic Acupuncture Stimulator SDZ-IIB Health Care Device (Nanjing Jisheng Medical Technology Co., Ltd., Nanjing, China). Rabbits were restrained in a specialized rabbit fixation box. Bilateral ocular acupoints, including Jingming (BL-1), Cuanzhu (BL-2), Sizhukong (TE-23), Tongziliao (GB-1), and Taiyang (EX-HN5), were selected for EA stimulation. Acupuncture needles (0.3 mm diameter, 15 mm length; Hwato) were inserted subcutaneously to a 5 mm depth. EA was delivered with a sparse-dense wave (2 Hz/20 Hz), 0.2 ms pulse width, and 1 mA intensity (adjusted to elicit slight muscle twitching at the insertion site). The positive electrode of the EA device was connected to Jingming (BL-1), and the negative electrode to the ipsilateral Taiyang (EX-HN5). EA stimulation was applied for 20 min per day.

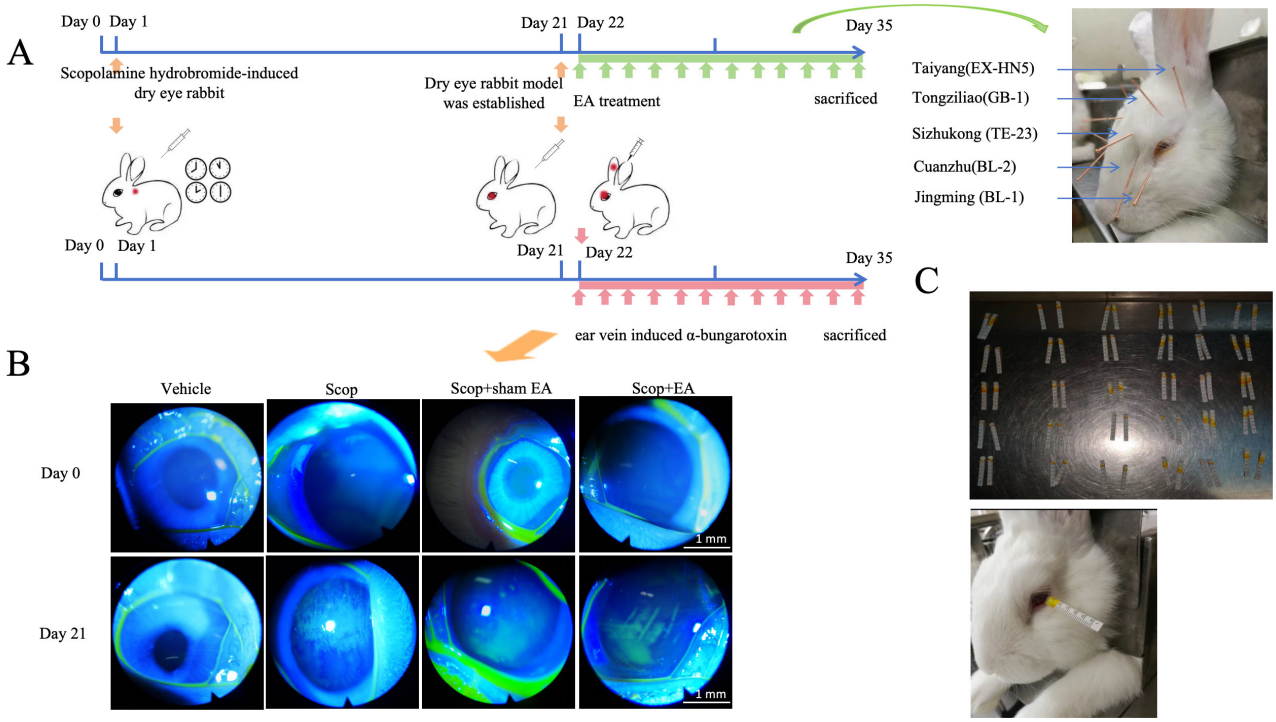

Fig. 1. Schematic diagram of the experimental principle. (A) Adult New Zealand white rabbits received four daily subcutaneous injections of Scop for 21 consecutive days. From day 22, EA stimulation was applied to bilateral ocular acupoints Jingming (BL-1), Cuanzhu (BL-2), Sizhukong (TE-23), Tongziliao (GB-1), Taiyang (EX-HN5). And α-BGT was injected via the ear vein for 14 days. (B) Experimental groups included the Vehicle control group, Scop-treated group, Scop-treated + sham EA group, and Scop-treated + EA group. By day 21, all groups except the Vehicle control group showed strong positive corneal FL staining, confirming successful establishment of the DED model (The magnification of the slit lamp lens is 10×). Scale bar = 1 mm. (C) SIT was measured in New Zealand white rabbits. EA, electroacupuncture; α-BGT, α-Bungarotoxin; FL, fluorescein.

2.5 Corneal FL

A corneal staining filter paper strip was placed into the lower eyelid fornix of the rabbit and moistened. FL was evenly distributed over the cornea through blinking. Corneal epithelial damage was graded using a cobalt blue filter. The cornea was divided into four quadrants, with scoring criteria as follows: 0 (no staining), 1 (<5 staining spots), 2 (>5 staining spots), and 3 (large-area FL plaques). The total score was the sum of scores from the four quadrants, with a maximum of 12 points.

2.6 Breakup Time of Tear Film

After moistening the FL sodium staining paper, it was gently touched to the conjunctival fornix of the lower eyelid 2–3 times. The rabbit was encouraged to blink several times to facilitate complete diffusion and distribution of the dye across the ocular surface. Under a slit lamp (Chongqing Shang Bang Medical Equipment Co., Ltd., Chongqing, China), the timer recorded the time of the first corneal dry spot, repeatedly measured three times, and the average time was used.

2.7 Schirmer I Test (SIT)

One end of the Schirmer strip was folded and inserted into the space between the middle and outer one-third of the lower eyelid and left in place for 5 min. The wet length of the strip was recorded after the strip was taken out (Fig. 1C).

2.8 Tear Osmolarity

Tear samples (20–50 µL) were collected from the lateral palpebral fissure (lacrimal lake) using a glass microcapillary pipette. Tear osmolarity was measured using the Vapro 5600 Osmometer (Wescor Inc., South Logan, UT, USA).

2.9 Histological Assessment

After the experimental protocol, animals were euthanized for the collection of corneas, lacrimal glands, and conjunctivae. These excised tissues were subsequently fixed in 4% paraformaldehyde, embedded in paraffin, sectioned at 5 µm, dried, and stained with hematoxylin and eosin. Histological changes were assessed under light microscopy.

2.10 Enzyme-Linked Immunosorbent Assay

A portion of the conjunctival tissue was excised, rinsed thoroughly with physiological saline, and weighed. Then the tissue was homogenized under ice bath conditions. Subsequently, the homogenate was diluted with 300 µL physiological saline and centrifuged, after which the supernatant was collected. A cholinesterase inhibitor (neostigmine, 10 µM) was added during tissue collection/homogenization. Samples were kept on ice, and assays were completed within 2 h of homogenization. The concentrations of ACh (JEB-14586; Nanjing Jin Yibai, China) and α7nAChR (JEB-14612) were determined using specific assay kits. The levels of ACh and α7nAChR were quantified using an enzyme-linked immunosorbent assay reader.

2.11 Immunohistochemistry

Conjunctival tissues were processed for embedding and sectioning, followed by antigen retrieval and blocking. Sections were incubated with a primary anti-HMGB1 antibody (1:500, GB11103-100; Servicebio, Wuhan, China) at 4 °C overnight, followed by incubation with horseradish peroxidase (HRP)-conjugated goat anti-rabbit IgG secondary antibody (1:1000, RS0002; ImmunoWay, San Jose, CA, USA) and staining with 3,3′-diaminobenzidine. Nuclei were counterstained with hematoxylin. Using Image-Pro Plus 6.0 software (National Institutes of Health, Bethesda, MD, USA), the integrated optical density (IOD) of positive staining and pixel area were measured, and the areal density was calculated as IOD/area.

2.12 Immunofluorescence Staining

Conjunctival paraffin sections were dewaxed through a standard xylene-ethanol gradient and rehydrated. After antigen retrieval (citrate buffer, pH 6.0, 95 °C for 20 min) and blocking in 5% goat serum (room temperature, 30 min), sections were divided into two groups for single-labeling detection. Then the sections were incubated overnight at 4 °C with primary antibodies against HMGB1 (1:300, GB11103-100; Servicebio) and α7nAChR (1:300, 144730; LSBio, Seattle, WA, USA). After three washes with phosphate-buffered saline (5 min each), the sections were incubated with Alexa Fluor® 488-conjugated goat anti-rabbit IgG H&L (1:1000, ab150077; Abcam, Cambridge, MA, USA) at room temperature for 1 h. Nuclei were counterstained with DAPI for 5 min. Sections were mounted with anti-fade mounting medium and observed under a fluorescence microscope (Olympus, Tokyo, Japan), with images captured using a consistent exposure time.

2.13 Periodic-Acid Schiff Staining

Conjunctival paraffin sections were dewaxed and stained with Periodic-acid Schiff reagent to highlight intracellular stored mucus and the secretory products of goblet cells. Positively stained goblet cells in the conjunctiva were counted, and the distance between the first and last goblet cells was measured to calculate the average number of goblet cells per millimeter.

2.14 Transmission Electron Microscopy

Initial fixation was conducted in 0.1 mol/L phosphate buffer (pH 7.4) with 2.5% glutaraldehyde, followed by post-fixation in 1% osmium tetroxide. After dehydration through an ascending series of alcohols, the samples were embedded in epoxy resin. Then, small blocks (1 mm^3) were excised from the central region of the conjunctiva. These blocks were subjected to double staining with lead acetate and uranyl acetate, after which they were observed under a transmission electron microscope.

2.15 Western Blot Analysis

Equal amounts of cell lysates were extracted from the conjunctiva, and the protein concentration was determined using the BCA protein assay. Protein was resolved by 10% sodium dodecyl sulfate polyacrylamide gel electrophoresis, electrotransferred to a PVDF membrane (Millipore, Burlington, MA, USA), blocked in 5% nonfat dry milk, and incubated overnight at 4 °C with the following primary antibodies: anti-HMGB1 rabbit polyclonal antibody (1:1000, GB11103, Servicebio) , anti-α7nAChR rabbit monoclonal antibody (1:1000, 144730, LSBio), and GAPDH rabbit monoclonal antibody (1:1000, 5174S; Cell Signaling Technology, Danvers, MA, USA) for immunoblotting. After three washes with Tris-buffered saline containing 0.05% Tween 20 for 10 min each, the membrane was incubated with HRP-conjugated goat anti-rabbit IgG (1:1000, RS0002; ImmunoWay) for 1 h at room temperature. Band intensities were analyzed using Quantity One software v4.6.6 (Bio-Rad, Hercules, CA, USA).

2.16 RayBiotech Cytokine Quantification Array

Total protein was extracted from the conjunctiva, and the protein concentration was measured using the BCA protein assay. A rabbit cytokine quantification array (QAL-CYT-1 kit; RayBiotech, Inc., Norcross, GA, USA) was employed to detect the expression of 10 cytokines (interleukin 1α [IL-1α], IL-1β, IL-8, IL-17A, IL-21, leptin, macrophage inflammatory protein-1beta, matrix metalloproteinase 9 [MMP-9], neural cell adhesion molecule 1 [NCAM-1], tumor necrosis factor alpha [TNF-α]) in the conjunctiva, and the assay was repeated three times. Then the signal was scanned using a Cy3 excitation curve with the InnoScan 300 Microarray Scanner (Innopsys, Carbonne, France). Data analysis was performed using QAL-CYT-1 data analysis software (Q-Analyzer).

2.17 Statistical Analyses

All experimental procedures were performed in at least three independent replicates. All data are presented as the mean $\pm$ standard error of the mean. All continuous data were first tested for normality using the Shapiro-Wilk

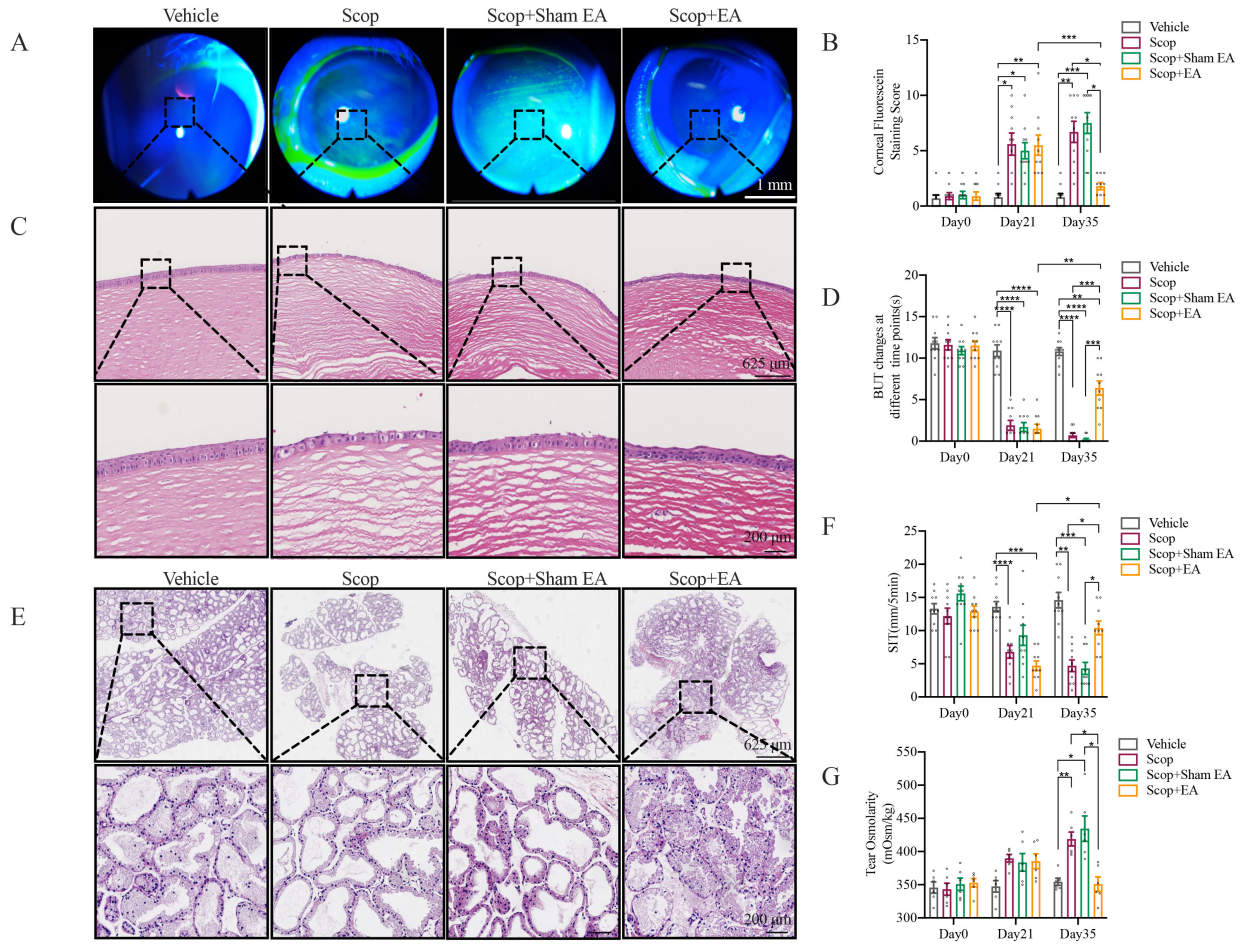

Fig. 2. EA stimulation alleviates ocular surface tissue damage and functional impairment in DED. (A) Representative images of corneal FL staining on day 35 (The magnification of the slit lamp lens is 10×). Scale bar = 1 mm. (B) Quantitative analysis of corneal FL staining scores (n = 10, Both eyes). (C) Representative hematoxylin and eosin (H&E) staining images of the cornea on day 35 (n = 3). Scale bars = 625 μm or 200 μm. (D) Quantitative analysis of the tear BUT (n = 10, Both eyes). (E) Representative H&E staining images of the lacrimal gland on day 35 (n = 3). Scale bars = 625 μm or 200 μm. (F) Quantitative analysis of tear flow (SIT, n = 10, Both eyes). (G) Quantitative analysis of tear osmolarity (n = 6). Data are presented as the mean ± standard error of the mean (SEM). Between-group comparisons: one-way ANOVA with Bonferroni correction. Within-group comparisons: paired *t*-tests with Bonferroni correction. *$p < 0.05$, **$p < 0.01$, ***$p < 0.001$, ****$p < 0.0001$. DED, dry eye disease; BUT, break-up time; SIT, Schirmer I test; ANOVA, one-way analysis of variance.

test and for homogeneity of variance using Levene's test. For data that conformed to a normal distribution and exhibited homogeneous variance, one-way analysis of variance (ANOVA) was used to compare the overall differences among multiple groups. If the main effect among groups was significant, further post-hoc analysis was performed with Bonferroni correction. For within-group comparisons, paired *t*-tests with Bonferroni correction were applied. Statistical significance was established for findings where both the uncorrected *p*-value was less than 0.05, and the corrected *p*-value remained less than 0.05 following adjustment for multiple comparisons. SPSS 22.0 software (IBM SPSS Inc., Armonk, NY, USA) was used for statistical analyses. $p < 0.05$ was considered statistically significant.

3. Results

3.1 EA Ameliorates Ocular Surface Functional Deficits and Tear Film Stability in DED

To determine whether EA stimulation can alleviate ocular surface functional abnormalities resulting from DED, a series of assessments was conducted following 3 and 5 weeks of continuous subcutaneous injection of Scop. At 3 and 5 weeks, the FL was elevated in the Scop and Scop + Sham EA groups compared to the Vehicle control group, indicating severe corneal epithelial damage in these Scop-treated groups. Concurrently, the BUT was significantly reduced in all three groups relative to the vehicle control group (Fig. 1B and Fig. 2B,D). After 5 weeks of Scop injection, the tear osmolarity was markedly increased, while

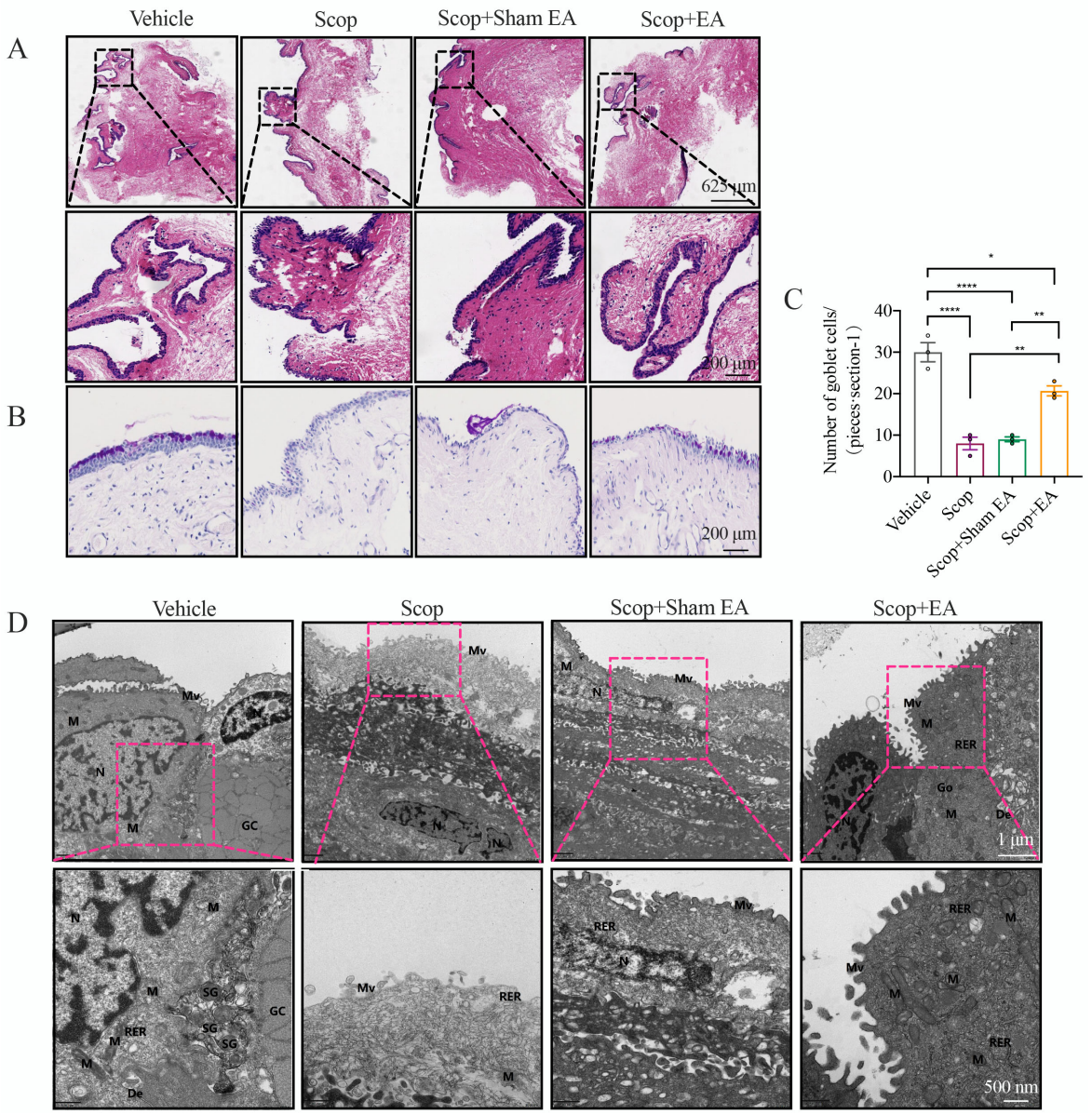

Fig. 3. EA stimulation modulates conjunctival tissue and ultrastructure in DED. (A) Conjunctival H&E staining on day 35 (n = 3). Scale bar = 625 μm. (B,C) Periodic-acid Schiff (PAS) staining of conjunctival goblet cells and counting of goblet cells in each group (n = 3). Scale bar = 200 μm. (D) Transmission electron microscopy of conjunctival epithelial cells, depicting microvilli (Mv), mitochondria (M), RER, nuclei (N), nucleoli (Nu), desmosomes (De), goblet cells (GCs), and secretory granules (SGs). Scale bars = 1 μm or 500 nm. Quantitative data are presented as the mean ± SEM, Between-group comparisons: one-way ANOVA with Bonferroni correction. *$p < 0.05$, **$p < 0.01$, ****$p < 0.0001$. RER, rough endoplasmic reticulum.

the SIT was significantly decreased in the Scop and Scop + Sham EA groups (Fig. 2A,B,D,F,G). EA stimulation for 2 weeks counteracted these adverse effects. These results suggest that EA exerts protective effects against corneal epithelial damage, consistent with the improved epithelial layer integrity observed in the histological sections (Fig. 2C). Additionally, EA alleviated ocular surface damage and mitigated ocular functional abnormalities induced by DED, with specific benefits in reducing tear osmolarity and enhancing tear film stability.

3.2 EA Contributes to the Amelioration of Pathological Tissue Damage in the Cornea, Lacrimal Glands, and Conjunctiva Induced by DED

The impact of EA stimulation on the mitigation of ocular surface tissue damage caused by DED was assessed by histopathological analysis. After 5 weeks of Scop injection, the corneal epithelial layers were diminished with superficial squamous epithelial cells sloughing off, accompanied by edema in the stromal layer and visible corneal epithelial shedding in the Scop and Scop + Sham EA groups. EA stimulation notably improved the corneal damage, ev-

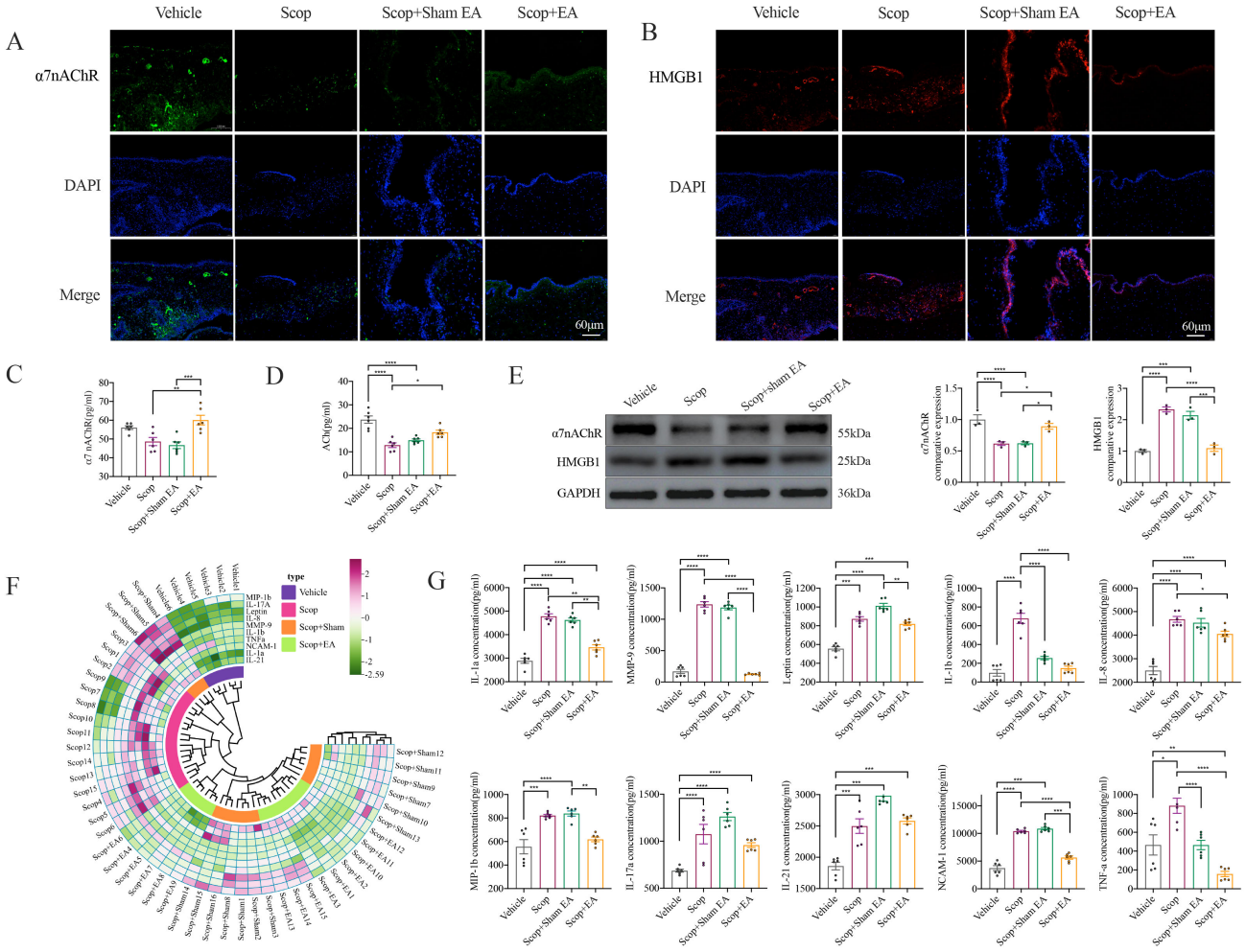

Fig. 4. EA stimulation suppresses Scop-induced conjunctival inflammation and activates α7nAChR. (A,B) The levels of α7nAChR and HMGB1 in conjunctival epithelial tissue were evaluated using immunofluorescence staining, Scale bar = 60 μm. (E) Western blotting (n = 3), respectively. (C,D) Expression of α7nAChR and ACh in conjunctival tissue was quantified using ELISA (n = 6). (F,G) A rabbit conjunctival protein array was utilized to analyze changes in cytokines and chemokines in the conjunctiva (n = 6), Cytokine circular heatmap (F), Expression of cytokines and chemokines in the conjunctiva (n = 6) (G). Quantitative data are presented as the mean ± SEM. Between-group comparisons: one-way ANOVA with Bonferroni correction. *$p < 0.05$, **$p < 0.01$, ***$p < 0.001$, ****$p < 0.0001$. α7nAChR, alpha-7 nicotinic acetylcholine receptor; HMGB1, high mobility group box 1; ELISA, Enzyme-Linked Immunosorbent Assay.

idenced by an increase in corneal layers, a less disordered structure of the superficial squamous epithelium, and a reduction in corneal epithelial shedding and stromal edema (Fig. 2A,C). The lacrimal glands, which primarily secrete the aqueous component of tears, displayed acinar atrophy and increased cavity size compared to the Vehicle control group in the Scop and Scop + Sham EA groups. EA stimulation attenuated the acinar atrophy (Fig. 2E). The conjunctival epithelial cells showed disrupted layers and polarity, with infiltration of lymphocytes and neutrophils, and partial epithelial cell detachment in the Scop and Scop + Sham EA groups. EA stimulation similarly ameliorated the conjunctival epithelial cells, with a decrease in epithelial cell detachment and a reduction in lymphocytes (Fig. 3A). Conjunctival goblet cells secrete conjunctival mucin to form the mucin layer of the tear film, which is pivotal for maintaining tear film stability and ocular surface homeostasis [23,24]. In comparison to the Vehicle control group, the Scop and Scop + Sham EA groups notably decreased the number of conjunctival goblet cells, whereas EA stimulation increased the number of goblet cells (Fig. 3B,C).

3.3 EA Stimulation Ameliorates the Ultrastructural Abnormalities in Conjunctival Tissue

The ultrastructural integrity of conjunctival epithelial cells was assessed in the Vehicle control group, revealing a pattern of short-columnar arrangement with uniform cytoplasmic density, continuous cell membrane structures, and the presence of microvilli along the membranes. The mi-

tochondrial membranes displayed elevated density, and the rough endoplasmic reticulum (RER) exhibited no signs of dilation, with ribosomes firmly anchored to its surface. Intercellular bridges were observed, and no significant widening of the intercellular spaces was noted. A profusion of secretory granules was evident adjacent to the goblet cells. By contrast, the Scop group displayed flattened cells with necrotic outermost layers. The cell membranes had microvilli, but the cytoplasm was sparse and disintegrating with a diminished number of organelles. Mitochondria were swollen, the membrane appeared blurred, and the matrix and cristae were slightly sparse. Intermediate layer cells were in a state of contraction, with a higher cytoplasmic density and increased intercellular space. The Scop + Sham EA group exhibited flattened cells, with microvilli attached to the membranes, and nuclei were elongated, with minimal accumulation of heterochromatin at the margins and a blurred nuclear membrane. Mitochondria were swollen, with a slightly sparse matrix and cristae, and the RER showed slight dilation with sparse ribosomes on its surface. Deeper-layer cells appeared contracted, with widened intercellular spaces. The Scop + EA group showed cells arranged in a short-columnar pattern, with uniform distribution of the cytoplasm. The cell membrane was intact, but microvilli were sparsely distributed. Nuclei showed a slight concavity, with heterochromatin aggregating in small patches and a clear nuclear membrane. Mitochondria were swollen, with intact membranes and slight dissolution of the matrix and cristae. The Golgi apparatus was not noticeably hypertrophied, and intercellular bridges were visible, with some local intercellular spaces slightly widened (Fig. 3D).

3.4 EA Stimulation Upregulates α7nAChR and ACh Expression While Downregulating HMGB1 in Conjunctival Epithelial Tissue

Previous experimental studies have established the pivotal role of α7nAChR in the cholinergic anti-inflammatory pathway [25]. To determine the involvement of α7nAChR in the anti-inflammatory effects of EA stimulation, we quantified the expression levels of ACh in each group following EA stimulation. Following EA stimulation, compared to the Scop group, the expression of α7nAChR and ACh in conjunctival tissue was significantly upregulated, whereas Sham acupuncture did not elicit an increase (Fig. 4C,D). HMGB1 is released during inflammatory responses, and its excessive release can lead to further cell damage and the release of HMGB1, exacerbating the inflammatory cascade. Immunofluorescence and Western blotting were utilized to detect α7nAChR and HMGB1 in conjunctival epithelial tissue, which are pivotal regulators of inflammatory factors. Scop-induced conjunctival epithelial tissue displayed reduced α7nAChR expression and increased HMGB1 expression, which EA stimulation effectively reversed (Fig. 4A,B,E).

3.5 Expression of α7nAChR in Conjunctival Tissue is Essential for the Anti-Inflammatory Effects of EA Stimulation

The conjunctiva represents the most metabolically active region of the ocular surface, serving as a critical interface for the immune response to a wide array of exogenous insults, including allergens, pathogens, and toxins. This mucosal epithelium forms the first line of defense in the ocular surface's innate and adaptive immune systems [26]. To elucidate the mechanism by which EA stimulation modulates inflammatory responses, we employed an antibody array to quantify the expression of a panel of 10 cytokines and chemokines. Compared to the Vehicle control group, the Scop-treated conjunctiva displayed pronounced upregulation of IL-1α, IL-1β, IL-8, IL-17A, IL-21, leptin, MMP-9, NCAM-1, and TNF-α. However, following EA stimulation, elevation in the expression of IL-1α, IL-1β, IL-8, MMP-9, NCAM-1, and TNF-α was significantly attenuated, signifying the marked inhibition of inflammation by EA stimulation, a response that was absent in the Scop + Sham EA group (Fig. 4F,G).

EA stimulation exerts its anti-inflammatory effects by stimulating the α7nAChR, which in turn suppresses the generation of pro-inflammatory cytokines within the conjunctival tissue. To investigate the role of α7nAChR in the EA-mediated anti-inflammatory response, we employed the specific α7nAChR antagonist α-BGT to block its activity. Intravenous injection of α-BGT via the ear vein reversed the EA-induced upregulation of α7nAChR expression, while the expression of ACh remained unaltered (Fig. 5A,B). Additionally, we re-evaluated the ocular surface phenotype of the Scop-induced dry eye rabbits following α-BGT treatment. This treatment abrogated EA stimulation's ability to (1) reduce corneal FL staining (Fig. 5C,E), (2) prolong tear BUT (Fig. 5F), (3) increase tear flow (Fig. 5H), (4) reduce tear osmolarity (Fig. 5I), and (5) mitigate corneal and lacrimal gland tissue damage (Fig. 5D,G). These data collectively indicate that EA stimulation elicits a localized activation of α7nAChR, which subsequently suppresses ocular surface inflammation and functional impairment.

3.6 The HMGB1 Signaling Pathway Mediated by α7nAChR in Conjunctival Tissue is Activated by EA Stimulation

To elucidate the potential cholinergic anti-inflammatory mechanism underlying EA stimulation, we examined whether the expression of HMGB1 and related pro-inflammatory cytokines and chemokines was inhibited following α-BGT blockade of α7nAChR expression. We observed that α-BGT reversed the beneficial effects of EA stimulation on conjunctival tissue damage, with a thinner epithelial layer and a corresponding decrease in the number of conjunctival goblet cells (Fig. 6A,B,F). Immunofluorescence and immunohistochemical assays

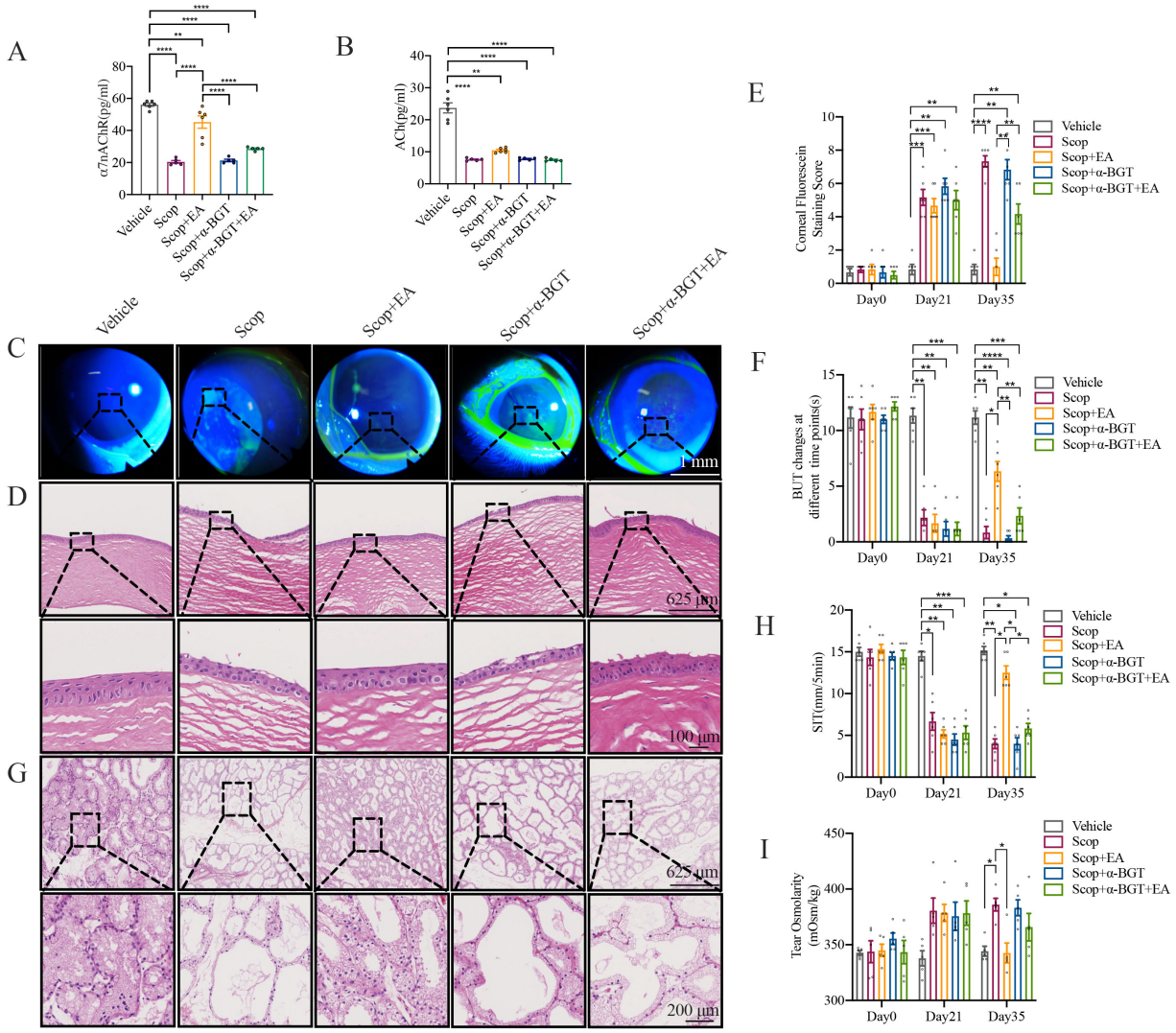

Fig. 5. EA stimulation mediates its anti-inflammatory effects through α7nAChR. (A,B) Expression of α7nAChR and ACh in conjunctival tissue was quantified using the enzyme-linked immunosorbent assay (n = 6). (C) Representative images of corneal FL staining on day 35, black arrow: Intense fluorescence indicates corneal epithelial defects (The magnification of the slit lamp lens is 10×). Scale bar = 1 mm. (D) Corneal H&E staining on day 35, black arrow: Corneal epithelial detachment and epithelial structural disorder; Blue arrow: Corneal stromal edema (n = 3). Scale bars = 625 μm or 100 μm. (E) Corneal FL staining score (n = 6). (F) Tear BUT (n = 6). (G) Lacrimal gland H&E staining on day 35 (n = 3). Scale bars = 625 μm or 200 μm. (H) Tear flow measurement (n = 6). (I) Tear osmolarity (n = 5). Quantitative data are presented as the mean ± SEM. Between-group comparisons: one-way ANOVA with Bonferroni correction. Within-group comparisons: paired *t*-tests with Bonferroni correction. $*p < 0.05$, $**p < 0.01$, $***p < 0.001$, $****p < 0.0001$.

were employed to assess the expression of α7nAChR and HMGB1 in conjunctival epithelium. α-BGT antagonist inhibited the EA-induced increase in α7nAChR expression, leading to an increase in HMGB1 expression (Fig. 6C–E,G). Although EA treatment resulted in a significant reduction in the levels of IL-1α, IL-1β, IL-8, MMP-9, NCAM-1, and TNF-α in the Scop g roup, these anti-inflammatory effects were not observed in the α-BGT group. Conversely, following treatment with the α-BGT antagonist, the inhibitory effects of EA on the total expression levels of IL-1β, IL-8, MMP-9, and TNF-α were not completely abolished (Fig. 6H,I). These findings indicate that EA suppresses the HMGB1 pathway by enhancing α7nAChR expression in conjunctival tissue to control inflammation. However, the regulatory effects of EA on IL-1β, IL-8, MMP-9, and TNF-α are not entirely mediated by the α7nAChR-dependent signaling pathway.

4. Discussion

This study investigated the ocular surface protective effects of EA stimulation and its potential mechanisms in a Scop-induced dry eye model. Our research yielded two

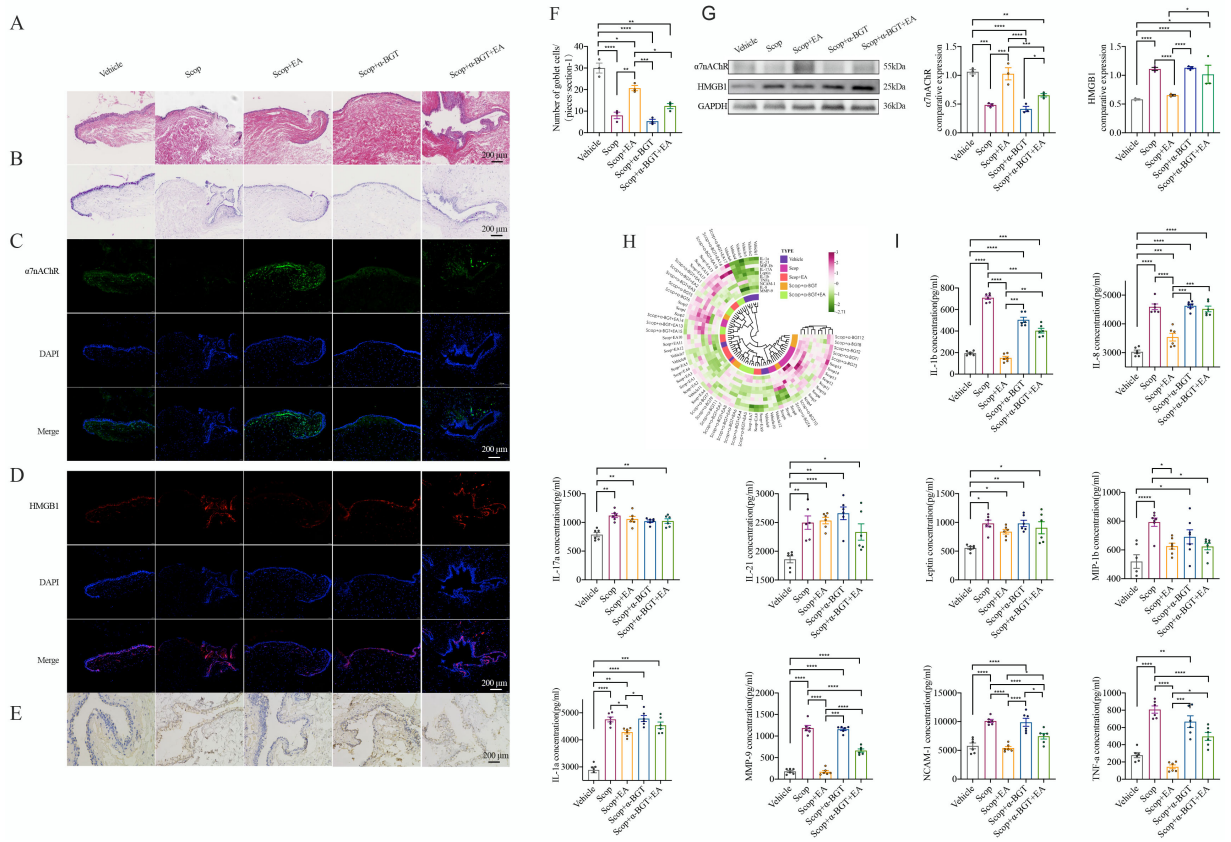

Fig. 6. EA stimulation engages the α7nAChR-mediated HMGB1 pathway in conjunctival tissue, suppressing inflammation. (A) H&E staining of the conjunctiva on day 35 (n = 3). (B) PAS staining for conjunctival goblet cells. (C,D) Immunofluorescence assays to determine the expression levels of α7nAChR and HMGB1 in the conjunctival epithelial layer. (E) Immunohistochemical analysis for assessing HMGB1 expression in the conjunctival epithelial tissue. (F) Quantification of goblet cell counts across different groups (n = 3). (G) Western blotting to evaluate the protein expression of α7nAChR and HMGB1 in the conjunctival epithelial tissue (n = 3). (H) Heatmap depicting the alterations in cytokine and chemokine profiles in rabbit conjunctival cells, as detected by protein microarray (n = 6). (I) Expression profiling of conjunctival cytokines and chemokines (n = 6). Statistical data are expressed as the mean $\pm$ SEM. Between-group comparisons: one-way ANOVA with Bonferroni correction. Scale bar = 200 µm. Statistical significance is indicated by $^{*}p < 0.05$, $^{**}p < 0.01$, $^{***}p < 0.001$, and $^{****}p < 0.0001$.

principal conclusions. First, EA was found to ameliorate ocular surface functional damage and tissue injury in the cornea, lacrimal glands, and conjunctiva induced by DED. Second, our data provide compelling evidence that conjunctival damage in DED is associated with dysregulation of α7nAChR, and the improvement in conjunctival tissue damage may be attributed to regulation of the α7nAChR/HMGB1 inflammatory pathway.

DED is a multifactorial ocular surface disorder involving conjunctival goblet cells, lacrimal glands, and meibomian glands. The coordinated function of these structures is critical for maintaining the electrolyte, water, mucin, and lipid composition of the tear film; dysfunction of these structures can lead to tear film instability, hyperosmolarity, and inflammation [27]. Typically, the blinking reflex refreshes the tear film at a rate of 5–10 times per minute, evenly distributing the tear film across the ocular surface and promoting the release of lipids from the meibomian glands. Prolonged interblink intervals or increased tear evaporation due to environmental factors can result in elevated tear osmolarity [28]. Elevated tear osmolarity is a hallmark of all forms of DED and is positively correlated with tear film instability [29] and the severity of DED [30,31]. Tear hyperosmolarity interacts with inflammation, activating downstream inflammatory cascades and exacerbating tear film instability [4,24,32]. The present study demonstrated that Scop-induced DED is associated with significantly elevated tear osmolarity, concurrent ocular surface functional damage, and tear film instability. Furthermore, we detected upregulated protein expression of HMGB1 and its downstream factors, including IL-1α, IL-1β, IL-8, IL-17A, IL-21, leptin, MMP-9, NCAM-1, and TNF-α, in conjunctival tissue. Molina-Leyva *et al.* [33] observed that the levels of inflammatory cytokines such as IL-1, IL-2, IL-6, IL-8, and TNF-α in the tears and conjunctival epithelium of patients with DED are higher than those

in healthy individuals, and these levels are positively correlated with the severity of DED. IL-1 signaling has been identified as a critical step in the differentiation of T helper 17 (Th17) cells, which are implicated in the development of autoimmune diseases and initiate downstream inflammatory cascade signaling [34]. Th17 cells are associated with the pathogenesis of many autoimmune diseases, including DED. IL-17, the signature cytokine of Th17 cells, promotes DED by disrupting the corneal epithelial barrier. A clinical study found a correlation between tear leptin concentration and DED symptoms and signs [35], which may be explained by leptin acting as an inflammatory factor; its increased concentration accelerates mitosis of cells around the ocular surface damage area, thereby regulating and promoting corneal epithelial cell regeneration. Notably, the activation of HMGB1 signaling is involved in the upregulation of inflammatory cytokines.

According to traditional Chinese medicine theory, periocular acupuncture is commonly used to treat various head and ocular conditions. Modern neuroanatomy shows that the acupoints Jingming (BL-1), Cuanzhu (BL-2), Sizhukong (TE-23), Tongziliao (GB-1), and Taiyang (EX-HN5) are located within the distribution of the ophthalmic branch of the trigeminal nerve. Stimulation of these acupoints can trigger excitatory signals in the brain via the trigeminal nerve, potentially improving visual function [36]. Clinical evidence suggests that acupuncture is more effective than artificial tears for DED treatment [37,38]. Zhao *et al*. [39] reported that periocular acupuncture modulates the serum levels of TNF-α, TGF-β, and IL-1 in patients with DED, thereby promoting the recovery of tear secretion function. In our previous work, we demonstrated that EA stimulation significantly alleviates ocular surface damage in DED. In the current study, we further observed that periocular EA stimulation markedly ameliorates ocular surface functional damage in Scop-induced dry eye rabbits, enhances ocular surface tissue integrity, and reduces tear osmolarity. Additionally, EA stimulation was found to increase the number of conjunctival goblet cells, improve the ultrastructure of the conjunctiva, downregulate HMGB1 expression in conjunctival epithelial tissue, and decrease the levels of IL-1α, IL-1β, IL-8, MMP-9, NCAM-1, and TNF-α. These findings indicate that the mechanism by which EA stimulation counteracts Scop-induced DED may be associated with the inhibition of HMGB1 signaling.

The α7nAChR is widely recognized as a key member of the neuronal nAChR family and plays a crucial role in the cholinergic anti-inflammatory pathway—a systemic anti-inflammatory mechanism that primarily operates via α7nAChR-dependent stimulation of the vagus nerve [40,41]. As a critical component of the neuroimmune regulatory pathway, α7nAChR activation effectively reduces the release of pro-inflammatory cytokines, which are closely associated with inflammation, neuropathic pain [42], and various neurodegenerative and neurodevelopmental disorders [43]. ACh, a well-known component of cholinergic neurotransmitters, can interact with α7nAChR to activate downstream signaling pathways involved in cell proliferation and apoptosis [44,45]. Studies have shown that ACh promotes corneal wound healing and inhibits corneal matrix fibrosis [46]. Dias *et al*. [47] found a correlation between reduced ACh levels and DED severity, which is consistent with our finding that modulating ACh levels can alleviate DED symptoms. In the current study, the use of α-BGT—a specific α7nAChR antagonist—reversed the protective effects of EA stimulation on Scop-induced ocular surface dysfunction and tissue damage in DED.

Additionally, α-BGT significantly reduced the number of conjunctival goblet cells; upregulated HMGB1-related factors, including IL-1β, IL-8, MMP-9, and TNF-α in conjunctival tissue; and downregulated α7nAChR expression. A observation in our study is that although α-BGT could specifically block the HMGB1 pathway by antagonizing α7nAChR, it failed to completely antagonize the downstream inflammatory cytokines. Specifically, significant differences in the levels of IL-1β, IL-8, MMP-9, and TNF-α were still observed between the Scop+α-BGT+EA group and the Scop group. This phenomenon indicates that EA exerts its anti-inflammatory effect against dry eye disease through a multi-target and multi-pathway mechanism. Multiple studies have confirmed that EA inhibits inflammatory responses by activating the vagus nerve and its α7nAChR [48–50]. Wang *et al*. [22] reported that EA alleviates postoperative cognitive decline in elderly patients with lacunar cerebral infarction and patients with post-spinal surgery by downregulating HMGB1/NF-κB expression, thereby reducing the levels of IL-6 and IL-1β. Combined with previous studies, our findings suggest that α7nAChR in ocular surface tissues may serve as an upstream signaling molecule involved in Scop-induced ocular surface damage in DED. Furthermore, EA-mediated regulation of α7nAChR expression to inhibit HMGB1 may be one of the molecular mechanisms underlying the alleviation of ocular surface inflammation in DED.

Several limitations of the current study should be noted. First, we used a single pharmacologically induced DED model, which cannot fully recapitulate autoimmune or age-related DED. Future studies should employ additional models (e.g., benzalkonium chloride- or hormonal deficiency-induced DED) to validate the generalizability of our findings. Second, using rabbits as experimental animals has inherent limitations, particularly in antibody selection and validation for molecular experiments. For example, RT-PCR was not used to verify results due to gaps in species-specific gene databases—notably the absence of the rabbit α7nAChR gene. Thus, we used antibodies for cross-validation at the protein level to ensure the integrity and accuracy of our experimental methodology. Future studies should adopt a greater variety of animal models.

5. Conclusions

This study elucidated the effects and mechanisms of EA stimulation in Scop-induced DED. The results showed that EA promotes corneal epithelial repair, increases tear secretion, enhances goblet cell counts, and improves tear film stability. Importantly, α-BGT—a selective α7nAChR antagonist—reversed the protective effects of EA on the ocular surface, suggesting that the protective effect of EA on conjunctival tissue may be associated with the regulation of the α7nAChR-HMGB1 inflammatory pathway. Our findings validate the effectiveness of EA in DED treatment and explore its mechanisms of action, providing valuable insights for clinical interventions in DED.

Availability of Data and Materials

The data presented in this study are available on request from the corresponding author.

Author Contributions

ND and JZ contributed equally to this work as co–first authors. QBW and YCW conceived the study and designed the research protocol. ND and JZ drafted the manuscript. ND and JZ participated in the refinement of the research design (e.g., optimization of data presentation framework and experimental result interpretation logic) and drafted the manuscript. Data acquisition and analysis were performed by SJL, DDZ, XW, and MTH. Immunohistochemistry and immunofluorescence experiments were conducted by LZG and YFW. HXS and TYJ provided help and advice on the ELISA experiments. Figures and visualization were prepared by ND, JZ, and SJL. QBW and YCW critically revised the manuscript for important intellectual content. Figures and visualization were prepared by ND, JZ, and SJL, with ND and JZ involved in the analysis of experimental data presented in the figures to ensure accuracy and consistency with the research hypothesis. QBW and YCW supervised the project and approved the final version. All authors made substantial contributions to the study, reviewed the manuscript, and approved the final version. All authors contributed to editorial changes in the manuscript. All authors have participated sufficiently in the work and agreed to be accountable for all aspects of the work.

Ethics Approval and Consent to Participate

All animal procedures were performed following the 3R principles and approved by the Ethics Committee of Nanjing University of Chinese Medicine (NO: 201809A018).

Acknowledgment

We thank Ejear English Editing Service for providing linguistic editing and proofreading services for this manuscript.

Funding

This work was supported by the Youth Program of the National Natural Science Foundation of China (No.82305377, 82205259), National Natural Science Foundation of jiangsu (No.BK20230455), the Foundation Project of Jiangsu Provincial Association of Traditional Chinese Medicine (CYTF2024002, CYTF2024001), Jiangsu Health Vocational College School-level Scientific Research Project (YIXT-YZ202401).

Conflict of Interest

The authors declare no conflict of interest.

References

[1] Britten-Jones AC, Wang MTM, Samuels I, Jennings C, Stapleton F, Craig JP. Epidemiology and Risk Factors of Dry Eye Disease: Considerations for Clinical Management. Medicina. 2024; 60: 1458. https://doi.org/10.3390/medicina60091458.

[2] Mohamed HB, Abd El-Hamid BN, Fathalla D, Fouad EA. Current trends in pharmaceutical treatment of dry eye disease: A review. European Journal of Pharmaceutical Sciences. 2022; 175: 106206. https://doi.org/10.1016/j.ejps.2022.106206.

[3] Bu J, Liu Y, Zhang R, Lin S, Zhuang J, Sun L, *et al*. Potential New Target for Dry Eye Disease-Oxidative Stress. Antioxidants. 2024; 13: 422. https://doi.org/10.3390/antiox13040422.

[4] Roucaute E, Huertas-Bello M, Sabater AL. Novel treatments for dry eye syndrome. Current Opinion in Pharmacology. 2024; 75: 102431. https://doi.org/10.1016/j.coph.2024.102431.

[5] Li S, Lu Z, Huang Y, Wang Y, Jin Q, Shentu X, *et al*. Anti-Oxidative and Anti-Inflammatory Micelles: Break the Dry Eye Vicious Cycle. Advanced Science. 2022; 9: e2200435. https://doi.org/10.1002/advs.202200435.

[6] Stanton E, Won P, Manasyan A, Gurram S, Gilllenwater TJ, Yenikomshian HA. Neuropathic pain in burn patients - A common problem with little literature: A systematic review. Burns. 2024; 50: 1053–1061. https://doi.org/10.1016/j.burns.2024.02.013.

[7] Wang M, Liu W, Ge J, Liu S. The immunomodulatory mechanisms for acupuncture practice. Frontiers in Immunology. 2023; 14: 1147718. https://doi.org/10.3389/fimmu.2023.1147718.

[8] Dong M, Wang WQ, Chen J, Li MH, Xu F, Cui J, *et al*. Acupuncture Regulates the Balance of $CD4^+$ T Cell Subtypes in Experimental Asthma Mice. Chinese Journal of Integrative Medicine. 2019; 25: 617–624. https://doi.org/10.1007/s11655-018-3055-6.

[9] Tang Y, Wang T, Yang L, Zou X, Zhou J, Wu J, *et al*. Acupuncture for post-operative cognitive dysfunction: a systematic review and meta-analysis of randomized controlled trials. Acupuncture in Medicine. 2021; 39: 423–431. https://doi.org/10.1177/0964528420961393.

[10] Zhao H, Dong F, Li Y, Ren X, Xia Z, Wang Y, *et al*. Inhibiting ATG5 mediated autophagy to regulate endoplasmic reticulum stress and $CD4^+$ T lymphocyte differentiation: Mechanisms of acupuncture's effects on asthma. Biomedicine & Pharmacotherapy. 2021; 142: 112045. https://doi.org/10.1016/j.biopha.2021.112045.

[11] Prinz J, Maffulli N, Fuest M, Walter P, Hildebrand F, Migliorini F. Acupuncture for the management of dry eye disease. Frontiers of Medicine. 2022; 16: 975–983. https://doi.org/10.1007/s11684-022-0923-4.

[12] Wu M, Tang Q, Gao W, Zhu L. A novel approach to the immediate effects of electroacupuncture on dry eye: A case series.

Explore. 2024; 20: 430–433. https://doi.org/10.1016/j.explore.2023.10.010.

[13] Ding N, Wei Q, Deng W, Sun X, Zhang J, Gao W. Electroacupuncture Alleviates Inflammation of Dry Eye Diseases by Regulating the α7nAChR/NF-κB Signaling Pathway. Oxidative Medicine and Cellular Longevity. 2021; 2021: 6673610. https://doi.org/10.1155/2021/6673610.

[14] Ding N, Wei Q, Xu Q, Liu C, Ni Y, Zhao J, *et al*. Acupuncture Alleviates Corneal Inflammation in New Zealand White Rabbits with Dry Eye Diseases by Regulating α7nAChR and NF-κB Signaling Pathway. Evidence-based Complementary and Alternative Medicine. 2022; 2022: 6613144. https://doi.org/10.1155/2022/6613144.

[15] Song JG, Li HH, Cao YF, Lv X, Zhang P, Li YS, *et al*. Electroacupuncture improves survival in rats with lethal endotoxemia via the autonomic nervous system. Anesthesiology. 2012; 116: 406–414. https://doi.org/10.1097/ALN.0b013e3182426ebd.

[16] Song Q, Hu S, Wang H, Lv Y, Shi X, Sheng Z, *et al*. Electroacupuncturing at Zusanli point (ST36) attenuates pro-inflammatory cytokine release and organ dysfunction by activating cholinergic anti-inflammatory pathway in rat with endotoxin challenge. African Journal of Traditional, Complementary, and Alternative Medicines. 2014; 11: 469–474. https://doi.org/10.4314/ajtcam.v11i2.35.

[17] Zhang L, Wu Z, Zhou J, Lu S, Wang C, Xia Y, *et al*. Electroacupuncture Ameliorates Acute Pancreatitis: A Role for the Vagus Nerve-Mediated Cholinergic Anti-Inflammatory Pathway. Frontiers in Molecular Biosciences. 2021; 8: 647647. https://doi.org/10.3389/fmolb.2021.647647.

[18] Zhang XF, Xiang SY, Geng WY, Cong WJ, Lu J, Jiang CW, *et al*. Electro-acupuncture regulates the cholinergic anti-inflammatory pathway in a rat model of chronic obstructive pulmonary disease. Journal of Integrative Medicine. 2018; 16: 418–426. https://doi.org/10.1016/j.joim.2018.10.003.

[19] Lema C, Reins RY, Redfern RL. High-Mobility Group Box 1 in Dry Eye Inflammation. Investigative Ophthalmology & Visual Science. 2018; 59: 1741–1750. https://doi.org/10.1167/iovs.17-23363.

[20] Ibrahim SM, Al-Shorbagy MY, Abdallah DM, El-Abhar HS. Activation of α7 Nicotinic Acetylcholine Receptor Ameliorates Zymosan-Induced Acute Kidney Injury in BALB/c Mice. Scientific Reports. 2018; 8: 16814. https://doi.org/10.1038/s41598-018-35254-1.

[21] Mei Z, Tian X, Chen J, Wang Y, Yao Y, Li X, *et al*. α7 nAchR agonist GTS 21 reduces radiation induced lung injury. Oncology Reports. 2018; 40: 2287–2297. https://doi.org/10.3892/or.2018.6616.

[22] Wang Z, Liu T, Yin C, Li Y, Gao F, Yu L, *et al*. Electroacupuncture Pretreatment Ameliorates Anesthesia and Surgery-Induced Cognitive Dysfunction via Activation of an α7-nAChR Signal in Aged Rats. Neuropsychiatric Disease and Treatment. 2021; 17: 2599–2611. https://doi.org/10.2147/NDT.S322047.

[23] Baudouin C, Rolando M, Benitez Del Castillo JM, Messmer EM, Figueiredo FC, Irkec M, *et al*. Reconsidering the central role of mucins in dry eye and ocular surface diseases. Progress in Retinal and Eye Research. 2019; 71: 68–87. https://doi.org/10.1016/j.preteyeres.2018.11.007.

[24] Bron AJ, de Paiva CS, Chauhan SK, Bonini S, Gabison EE, Jain S, *et al*. TFOS DEWS II pathophysiology report. The Ocular Surface. 2017; 15: 438–510. https://doi.org/10.1016/j.jtos.2017.05.011.

[25] Szczesna-Iskander DH. Post-blink tear film dynamics in healthy and dry eyes during spontaneous blinking. The Ocular Surface. 2018; 16: 93–100. https://doi.org/10.1016/j.jtos.2017.09.002.

[26] de Paiva CS, St Leger AJ, Caspi RR. Mucosal immunology of the ocular surface. Mucosal Immunology. 2022; 15: 1143–1157. https://doi.org/10.1038/s41385-022-00551-6.

[27] Lam H, Bleiden L, de Paiva CS, Farley W, Stern ME, Pflugfelder SC. Tear cytokine profiles in dysfunctional tear syndrome. American Journal of Ophthalmology. 2009; 147: 198–205. e1. https://doi.org/10.1016/j.ajo.2008.08.032.

[28] Peng CC, Cerretani C, Braun RJ, Radke CJ. Evaporation-driven instability of the precorneal tear film. Advances in Colloid and Interface Science. 2014; 206: 250–264. https://doi.org/10.1016/j.cis.2013.06.001.

[29] Liu H, Begley C, Chen M, Bradley A, Bonanno J, McNamara NA, *et al*. A link between tear instability and hyperosmolarity in dry eye. Investigative Ophthalmology & Visual Science. 2009; 50: 3671–3679. https://doi.org/10.1167/iovs.08-2689.

[30] Tomlinson A, Khanal S, Ramaesh K, Diaper C, McFadyen A. Tear film osmolarity: determination of a referent for dry eye diagnosis. Investigative Ophthalmology & Visual Science. 2006; 47: 4309–4315. https://doi.org/10.1167/iovs.05-1504.

[31] Willcox MDP, Argüeso P, Georgiev GA, Holopainen JM, Laurie GW, Millar TJ, *et al*. TFOS DEWS II Tear Film Report. The Ocular Surface. 2017; 15: 366–403. https://doi.org/10.1016/j.jtos.2017.03.006.

[32] Baudouin C, Aragona P, Messmer EM, Tomlinson A, Calonge M, Boboridis KG, *et al*. Role of hyperosmolarity in the pathogenesis and management of dry eye disease: proceedings of the OCEAN group meeting. The Ocular Surface. 2013; 11: 246–258. https://doi.org/10.1016/j.jtos.2013.07.003.

[33] Molina-Leyva I, Molina-Leyva A, Bueno-Cavanillas A. Efficacy of nutritional supplementation with omega-3 and omega-6 fatty acids in dry eye syndrome: a systematic review of randomized clinical trials. Acta Ophthalmologica. 2017; 95: e677–e685. https://doi.org/10.1111/aos.13428.

[34] Na KS, Mok JW, Kim JY, Rho CR, Joo CK. Correlations between tear cytokines, chemokines, and soluble receptors and clinical severity of dry eye disease. Investigative Ophthalmology & Visual Science. 2012; 53: 5443–5450. https://doi.org/10.1167/iovs.11-9417.

[35] Hao R, Liu Y, Li XM. Leptin's concentration in tears and dry eye: a clinical observational study. International Journal of Ophthalmology. 2021; 14: 83–88. https://doi.org/10.18240/ijo.2021.01.12.

[36] Zhang X, Zhang B, Peng S, Zhang G, Ma J, Zhu W. Effectiveness of acupuncture at acupoint BL1 (Jingming) in comparison with artificial tears for moderate to severe dry eye disease: a randomized controlled trial. Trials. 2022; 23: 605. https://doi.org/10.1186/s13063-022-06486-4.

[37] Kim TH, Kang JW, Kim KH, Kang KW, Shin MS, Jung SY, *et al*. Acupuncture for the treatment of dry eye: a multicenter randomised controlled trial with active comparison intervention (artificial teardrops). PLoS ONE. 2012; 7: e36638. https://doi.org/10.1371/journal.pone.0036638.

[38] Liu Q, Liu J, Ren C, Cai W, Wei Q, Song Y, *et al*. Proteomic analysis of tears following acupuncture treatment for menopausal dry eye disease by two-dimensional nano-liquid chromatography coupled with tandem mass spectrometry. International Journal of Nanomedicine. 2017; 12: 1663–1671. https://doi.org/10.2147/IJN.S126968.

[39] Zhao J, Xue SY, Wang SC, Pan X H, Xu J, Lin CM. Randomized Controlled Trial of Effect of Acupuncture on Inflammatory Factors in Patients with Xerophthalmia. Chinese Archives of Traditional Chinese Medicine 2019, 37: 250–252. (In Chinese).

[40] Su X, Lee JW, Matthay ZA, Mednick G, Uchida T, Fang X, *et al*. Activation of the alpha7 nAChR reduces acid-induced acute lung injury in mice and rats. American Journal of Respiratory Cell and Molecular Biology. 2007; 37: 186–192. https://doi.org/10.1165/rcmb.2006-0240OC.

[41] Wang H, Liao H, Ochani M, Justiniani M, Lin X, Yang L, *et al*. Cholinergic agonists inhibit HMGB1 release and improve survival in experimental sepsis. Nature Medicine. 2004; 10: 1216–1221. https://doi.org/10.1038/nm1124.

[42] Hone AJ, McIntosh JM. Nicotinic acetylcholine receptors in neuropathic and inflammatory pain. FEBS Letters. 2018; 592: 1045–1062. https://doi.org/10.1002/1873-3468.12884.

[43] Dineley KT, Pandya AA, Yakel JL. Nicotinic ACh receptors as therapeutic targets in CNS disorders. Trends in Pharmacological Sciences. 2015; 36: 96–108. https://doi.org/10.1016/j.tips.2014.12.002.

[44] Kurzen H, Wessler I, Kirkpatrick CJ, Kawashima K, Grando SA. The non-neuronal cholinergic system of human skin. Hormone and Metabolic Research. 2007; 39: 125–135. https://doi.org/10.1055/s-2007-961816.

[45] Wessler I, Kirkpatrick CJ, Racké K. The cholinergic 'pitfall': acetylcholine, a universal cell molecule in biological systems, including humans. Clinical and Experimental Pharmacology & Physiology. 1999; 26: 198–205. https://doi.org/10.1046/j.1440-1681.1999.03016.x.

[46] Słoniecka M, Danielson P. Acetylcholine decreases formation of myofibroblasts and excessive extracellular matrix production in an in vitro human corneal fibrosis model. Journal of Cellular and Molecular Medicine. 2020; 24: 4850–4862. https://doi.org/10.1111/jcmm.15168.

[47] Dias AC, Módulo CM, Jorge AG, Braz AM, Jordão AA, Jr, Filho RB, *et al*. Influence of thyroid hormone on thyroid hormone receptor beta-1 expression and lacrimal gland and ocular surface morphology. Investigative Ophthalmology & Visual Science. 2007; 48: 3038–3042. https://doi.org/10.1167/iovs.06-1309.

[48] Chi L, Du K, Liu D, Bo Y, Li W. Electroacupuncture brain protection during ischemic stroke: A role for the parasympathetic nervous system. Journal of Cerebral Blood Flow and Metabolism. 2018; 38: 479–491. https://doi.org/10.1177/0271678X17697988.

[49] Wang Z, Hou L, Yang H, Ge J, Wang S, Tian W, *et al*. Electroacupuncture Pretreatment Attenuates Acute Lung Injury Through α7 Nicotinic Acetylcholine Receptor-Mediated Inhibition of HMGB1 Release in Rats After Cardiopulmonary Bypass. Shock. 2018; 50: 351–359. https://doi.org/10.1097/SHK.0000000000001050.

[50] Zhang J, Yong Y, Li X, Hu Y, Wang J, Wang YQ, *et al*. Vagal modulation of high mobility group box-1 protein mediates electroacupuncture-induced cardioprotection in ischemia-reperfusion injury. Scientific Reports. 2015; 5: 15503. https://doi.org/10.1038/srep15503.